Violation of Electrostatic Rules: Shifting Balance between Pnicogen Bond and Lone Pair-π Interaction Tuned by Substituents

Zongqing Chi,[1] Tong Yan,[1] Qingzhong Li,[1,*] Steve Scheiner[2,*]

[1] The Laboratory of Theoretical and Computational Chemistry, School of Chemistry and Chemical Engineering, Yantai University, Yantai 264005, People's Republic of China

[2] Department of Chemistry and Biochemistry, Utah State University, Logan, UT 84322-0300, USA

***To whom all correspondence should be addressed**:

Corresponding authors: Qingzhong Li and Steve Scheiner

E-mail: liqingzhong1990@sina.com and steve.scheiner@usu.edu

Abstract

Complexes were formed pairing ZCl_3 (Z=P, As, Sb) with C_2R_4 (R = H, F, CN). The first interaction present is a pnicogen bond between the Z atom and the C=C π-bond. This bond weakens as the H atoms of ethylene are replaced by electron-withdrawing F and CN and the potential above the alkene switches from negative to positive. In the latter two cases, another set of noncovalent bonds is formed between the Cl lone pairs of ZCl_3 and the π*(C=C) antibonding orbital, as well as with the F or CN substituents. The growing strength of these interactions, coupled with a large dispersion energy, more than compensates for the weak pnicogen bond in $C_2(CN)_4$, with its repulsion between areas of positive charge on each subunit, making its complexes with ZCl_3 very strong, as high as 25 kJ/mol. The pnicogen bond in C_2F_4 is weaker than in C_2H_4, and its subsidiary lone pair-π bonds weaker than in $C_2(CN)_4$, so the complexes of this alkene with ZCl_3 are the weakest of the set.

Keywords: AIM; NBO; MEP; π-hole; Dispersion

1. Introduction

After a number of early indications that a pnicogen atom, i.e. P, As, Sb, might be able to engage in an attractive interaction with an electronegative atom on another molecule,[1-10] a number of papers appeared that elaborated on this concept. For example, it was found that the physicochemical properties of the products in some chemical reactions change significantly due to the presence of such interactions,[11-12] and they play a decisive role in some supramolecular self-assembly processes.[13-15] This idea picked up a head of steam in 2011 when a number of papers appeared that explored various aspects of this interaction, dubbed the pnicogen bond, more thoroughly.[16-21]

The pnicogen bond can be divided into σ-hole and π-hole interactions according to the distribution of the positive electrostatic potential on the pnicogen donor atom surface. The σ-hole is an area with positive electrostatic potential along the extension of a σ-bond from the pnicogen atom to a substituent. The positive electrostatic potential above and below a planar molecule such as NO_2X and PO_2X is commonly referred to as a π-hole.[22-23] The most common electron donor is a lone pair on a partner molecule, but metal hydrides,[24] radicals,[25] carbenes,[26] and π-systems[27-29] can also serve in this capacity. As an example, the pnicogen-π interaction in the $PCl_3\cdots C_6H_6$ dimer has been confirmed at low temperature by infrared spectroscopy.[27] The same sort of noncovalent bonding is relevant in biological systems and it may be involved in a mechanism of inhibiting Sb-based drugs for treating leishmaniasis.[28] An earlier work[29] compared the pnicogen bonds involving a range of different π electron donor molecules and found that the simple C=C double bond in ethylene is a stronger donor than acetylene but weaker than conjugated systems. An examination of substituent effects in $RH_2P\cdots C_2HM$ (R=H, OH, H_3C, NC, F; M=H, OH, CH_3, Li), noted electron-donating groups in the π electron donor amplify the pnicogen bond as do electron-withdrawing groups in the electron acceptor. These bonds are also subject to cooperative effects, as in the $RH\cdots FH_2Y\cdots C_2H_4$ (R=OH, NC, F; Y=P and As) triads.[30]

The lone pair-π (lp-π) designation refers to charge donation from a lone pair (lp) of one molecule into the π system of another, typically into a π* orbital. [31] The lp-π interaction is an important binding mode occurring in biomolecules[31-36] and plays a central role in stabilizing the structures of nucleic acids and proteins and modulating the recognition of protein DNA and enzyme substrates;[37-41] it has been recently reviewed in the full context of biological systems.[42]

The interaction is currently under extensive examination with a large number of studies conducted recently.[34, 43-49] As in the case of the pnicogen bond, the strength of the lp-π interaction is also sensitive to substituents. For instance, the lp-π interaction of water with hexafluorobenzene (8.8 kJ/mol) is stronger than that with benzene (2.5 kJ/mol).[50]

The existence of these two interactions raises an interesting question. Given the ability to engage in either a pnicogen bond or a lp-π interaction, which of the two would be preferred? What would be the circumstances that might lead to one or the other as the preferred binding mode, and are there occasions where a system could shift from one to the other? Can a set of rules be formulated that would allow one to predict in advance which interaction would be more stable?

In order to answer these questions, ethylene is taken as a very simple prototype π-electron system. Its π-system could donate electrons into a pnicogen bond, as has been shown previously,[29] or could serve as a sink of density from the lone pairs of a partner molecule. In order to examine substituent effects, the four H atoms of ethylene are replaced, first by the simple F atom, and then by the C≡N group, both strong electron-withdrawing agents. As a partner molecule, PCl_3 could participate in either of the two interactions under study. The P atom is expected to contain three σ-holes, one opposite each P-Cl bond, so can form a pnicogen bond with the alkene π-system. Each Cl atom contains three lone pairs, any of which can engage in a lp-π interaction with the alkene. As it is widely accepted that the strength of a pnicogen bond varies according to the size of the pnicogen atom, the P is replaced alternately by its heavier congeners As and Sb. There are thus a total of nine complexes examined here. Each of three ZCl_3 molecules (Z=P, As, Sb) is paired with each of three alkenes C_2H_4, C_2F_4, and $C_2(CN)_4$.

2. Computational Methods

The complexes and their monomers were first optimized at the MP2/aug-cc-pVDZ level and their nature as minima on the potential energy surface was confirmed by frequency calculations at the same level. To obtain more reliable results, these structures were then re-optimized at the MP2/aug-cc-pVTZ level. For the Sb atom, aug-cc-pVDZ-PP and aug-cc-pVTZ-PP pseudopotential basis sets were applied to account for relativistic effects.[51] The interaction energy was calculated as the difference in energy between the complex and the sum of the two monomers frozen in the same geometry as in the complex. This quantity was corrected for basis set superposition error (BSSE) by the counterpoise procedure proposed by Boys and Bernard.[52]

All calculations were performed using Gaussian 09 software.[53]

Molecular electrostatic potentials (MEPs) on the 0.001 au isosurface were calculated at the MP2/aug-cc-pVTZ(PP) level and their extrema were determined using the WFA-SAS (wave function analysis - surface analysis suite) procedure.[54] AIM2000 software was used to analyze the topological properties at each bond critical point (BCP).[55] Natural bond orbital (NBO) analysis was performed at the HF/aug-cc-pVTZ(PP) level by the NBO program contained within the Gaussian software.[56] NCI (non-covalent interaction) maps were plotted using the Multiwfn and VMD programs.[57-58] The LMOEDA (localized molecular orbital–energy decomposition analysis) method[59] using the GAMESS program[60] was used to decompose the interaction energy into electrostatic, exchange, repulsion, polarization and dispersion components.

3. Results and Discussion

3.1. MEP of Monomers

The character of the molecular electrostatic potential (MEP) provides strong indications as to how molecules will arrange themselves relative to one another within a dimer. The MEP of each of the monomers under study here is displayed in Figure 1. The most positive regions are indicated by blue, and negative by red. There is one σ-hole lying directly opposite each of the Z-Cl bonds of ZCl_3, with values at their maximum, $V_{s,max}$, varying from 0.045au for PCl_3 up to 0.073 au for $SbCl_3$. The electron-withdrawing nature of the Cl substituents draw density out of the Z lone pair, such that the MEP in its vicinity is positive, albeit much less so than the respective σ-hole of each molecule. For this reason, it is anticipated that a nucleophile ought to be drawn toward a σ-hole, rather than the less positive Z lone pair area.

Turning next to the $R_2C{=}CR_2$ systems on the right side of Fig 1, there is an interesting reversal of charge associated with changing R substituents. As noted earlier,[30] ethylene contains a negative blue region above the molecular plane, with $V_{s,min}$=-0.027 au. But the replacement of the four H atoms by the electron-withdrawing F or CN substituents pulls electron density out of this π-region, turning the blue region red, i.e. imparting to this area a positive MEP. CN is more effective than is F in this regard, leading to a larger red area, which would tend to repel an incoming positive σ-hole of another molecule.

3.2. Geometrics and Interaction Energies

Fig 2 depicts the general structures of the heterodimers derived from each of the different pairings of the monomers. The ZCl_3 molecule sits above the $R_2C{=}CR_2$ plane, with the Z atom

somewhat closer to one C atom (C_1) than to the other (C_2). C_1 lies approximately along the extension of the Z-Cl_1 bond, i.e. along its σ-hole. R_1 refers to the Z-C_1 distance, while the distances of the two other Cl atoms from C_2 are denoted R_2 and R_3, as illustrated in Fig 2. The angle between the C=C bond and the C_2-Z axis is termed α, while β refers to the alignment of C_1 along the Z-Cl_1 axis, θ(Cl_1-Z··C_1). All nine of the heterodimers are displayed more explicitly in Fig S1.

These geometrical parameters are reported in Table 1 where several trends are apparent. Despite the very different vdW radii of the three Z atoms, R_1, is fairly insensitive to the identity of Z, and even becomes smaller as Z grows larger for $H_2C=CH_2$. Cl_2 and Cl_3 lie a bit over 3 Å from C_2, and these distances contract a small amount in the order P > As > Sb. R_2 and R_3 are nearly equal for C_2F_4 and $C_2(CN)_4$, but there is much more asymmetry for ethylene, where these two distances differ by more than 0.2 Å. The α angle is less than 90° for $H_2C=CH_2$, placing the Z atom somewhat toward the C=C midpoint, but larger than 90° for the other two alkenes. This pattern is consistent with the negative region over the C=C midpoint for ethylene which would tend to attract the PCl_3 σ-hole, and the opposite for the two substituted alkenes with their negative MEP in that location. Note also the greater deviation of α from 90° for $C_2(CN)_4$ with its more extensive positive π MEP. The β angles all place the C_1 atom roughly along the extension of the Z-Cl_1 axis. The largest deviations from linearity tend to occur for the smaller Z atoms, which are the weakest pnicogen bonds, as detailed below.

The interaction energies contained in the second column of Table 1 manifest some interesting, and perhaps even counterintuitive trends. On one hand, replacement of the four H atoms of $H_2C=CH_2$ with electron-withdrawing substituent F reduces the interaction energy, whereas the CN substituent, also electron-withdrawing, increases this quantity. Another distinction arises with respect to the dependence on the size of the Z atom. The interaction energy for $H_2C=CH_2$ climbs in the order P < As < Sb, whereas the exact opposite pattern is associated with the other two alkenes. It is possible to reconcile these orders with the MEPs in Fig 1. The MEP above $H_2C=CH_2$ is negative, so its attraction for the Lewis acid ought to grow along with its increasing σ-hole. In contrast, the π MEPs of $F_2C=CF_2$ and $(NC)_2C=C(CN)_2$, are positive so can be expected to more strongly repel a growing positive σ-hole. In other words, the two types of alkenes behave in an opposite fashion simply because they have opposite charges in their π-regions. The latter argument based on repulsion, however, is unable to explain the overall

attractive interaction energy, particularly the large E^{int} for $(NC)_2C=C(CN)_2$.

3.3. Decomposition of Interaction Energy

Partitioning of the total interaction energy into physically meaningful components provides some insights into some of the trends above. Five such components: electrostatic (E^{ele}), exchange (E^{ex}), repulsion (E^{rep}), polarization (E^{pol}) and dispersion (E^{disp}), are reported in Table 2 for the nine heterodimers. Of greatest interest are the three attractive terms E^{ele}, E^{pol}, E^{disp}, with their percentage contribution to their sum indicated in parentheses.

First with respect to the electrostatic attraction, E^{ele} accounts for nearly 50% of the total for $H_2C=CH_2$ but this contribution drops to only about 25% for $F_2C=CF_2$ and still lower, below 20% for $(NC)_2C=C(CN)_2$. This diminution is consistent with the growing negative MEP in the π-regions, and its inability to attract a σ-hole as mentioned above. There is little to distinguish one complex from another with regard to E^{pol}, as this quantity remains in the 13-20% range for all structures. Dispersion, on the other hand, is evidence of a real difference between $H_2C=CH_2$ and its substituted derivatives. For any alkene, the absolute value of E^{disp} rises as the pnicogen atom grows in size, consistent with the greater number of electrons. But more importantly, while E^{disp} makes up no more than 43% for ethylene, its contribution is much larger for substituted $R_2C=CR_2$ where it accounts for more than 60% and even as high as 73% for $C_2(CN)_4\cdots SbCl_3$.

In summary, the energy component profile for the $H_2C=CH_2$ dimers fits the profile of a strongly electrostatic interaction, with a sizable secondary dispersion attractive energy. For the other two $R_2C=CR_2$ alkenes, however, their positive π-region reduces the electrostatic attraction to a small percentage, and the complexation relies instead on dispersion as its primary origin.

3.4. AIM and NCI analyses

The strength of specific intermolecular interactions can be assessed via analysis of the topology of the electron density, through AIM and NCI. The AIM molecular diagrams are exhibited in Fig S2, which indicate in all cases a pnicogen bond. The bond path begins at the Z atom, and terminates either at C_1 or at a point close to it along the C_1-C_2 axis. The values of the density, its Laplacian, and energy density for these paths are compiled in Table 3. The trends in these data are only partially consistent with the energetics in Table 1. For the unsubstituted ethylene, the increasing values of ρ and $\nabla^2\rho$ in the P < As < Sb sequence match the increasing interaction energy, as does the near insensitivity of all of these quantities to Z for C_2F_4. On the other hand, the particularly high interaction energies for $C_2(CN)_4$ are belied by the small values

of ρ. Based on AIM analysis, the pnicogen bond is rather weak in this latter series and their high interaction energies are derived from some other source.

A partial resolution of this issue arises in consideration of bonds other than the principal pnicogen bond. In the cases of the substituted $R_2C{=}CR_2$ molecules, there are also bond paths involving Cl_2 and Cl_3. These paths terminate at F atoms for C_2F_4 or at the C atom of the C≡N substituent for $C_2(CN)_4$. In the case of the latter alkene, there are also bond paths that lead to the approximate midpoint of the C=C bond. The values of the AIM parameters in Table 4 indicate these bonds are weaker than the principal $Z{\cdots}C_1$ pnicogen bond but neither are they negligible. Unlike the principal pnicogen bond parameters, the secondary values show little sensitivity to the nature of the Z atom. The BCP densities of the Cl···F bonds of C_2F_4 are about 0.046 au, less than half of the principal $Z{\cdots}C_1$ quantities. In comparison, the densities for Cl···C (of the C≡N substituent) are about 0.0065 au, only a little smaller than $Z{\cdots}C_1$. Added to these bonds for $C_2(CN)_4$ are another pair of bonds that connect the $AsCl_3$ and $SbCl_3$ Cl atoms with the C_1-C_2 midpoint. AIM assesses these bonds as comparable in strength to the Cl···C bonds. It appears that the multitude of bonds within the $C_2(CN)_4$ complexes is able to compensate for the weak pnicogen bond, to help explain their high total interaction energies.

The NCI analyses in Fig S3 echo the AIM bond paths and also adds weaker bonds involving the Cl atoms, even for C_2H_4 which were not present via AIM. With respect to the pnicogen bonds, the color change from green to blue in the transition from PCl_3 to $SbCl_3$ suggests a strengthening. In addition to the attractive interactions, NCI also indicates repulsive contacts as well, via the red colors in Fig S3.[61-62]

3.5. NBO analysis

An alternate view of the interactions between molecules considers transfers of charge between specific orbitals of each monomer via the NBO protocol. The lump sum total of charge transferred between the molecules is reported as CT in the first column of Table 5. The negative quantities for both C_2H_4 and C_2F_4 indicate that charge is transferred from the alkene to the Lewis acid ZCl_3, as would be expected for a pnicogen bond. For either alkene, note that this quantity increases along with the size of the Z atom. The charge flows in the opposite direction for $C_2(CN)_4$ with CT roughly equal to 0.02 e, larger in absolute value than for the preceding two alkenes.

The underlying reason for this curious reversal can be gleaned by considering a number of

the most important charge transfers between individual orbitals on the two subunits. E_1 represents the energetic consequence of charge transfer from the π(C=C) bond of the alkene to the σ*(Z-Cl_1) antibonding orbital, the traditional source of pnicogen bonding. E_2 and E_3 are similar but involve the Z-Cl_2 and Z-Cl_3 antibonding orbitals, which also are typically involved in related bonds, albeit by a lesser amount. As expected, the latter two terms are far smaller than E_1. Cumulatively, these three terms paint a picture of a pnicogen bond that is strongest for the unsubstituted ethylene, but becomes progressively weaker as H is replaced by F and then CN. This bond also strengthens as the Z atom grows larger, with an exception for $C_2(CN)_4$, for which the bond is weak, and gets even weaker for the heavier Z atoms.

The last two columns of Table 5 refer to back transfer, from the ZCl_3 molecule to the alkene π*(C=C) antibonding orbital. The charge originates on the Z lone pair for E_4, and on the Cl_3 lone pair for E_5. While these lp→π quantities are sizable, they are generally considerably smaller than E_1. But there is an exception in that E_4 exceeds E_1 for the complexes involving $C_2(CN)_4$.

A reasonable interpretation of Table 5 portrays the bonding as follows. The Z···π pnicogen is the dominating factor in the complexes that include ethylene and its perfluorinated derivative. There is a certain amount of reinforcement derived from back transfer into the π* orbital, but the former overwhelms the latter and the net charge direction is from alkene to ZCl_3. The pnicogen bond is considerably stronger for ethylene, and for either alkene the bond strengthens as the Z atom grows in size. In the case of $C_2(CN)_4$···ZCl_3, however, the pnicogen bond has weakened to the point that the lp→π back transfer becomes the larger factor, and net charge moves in the opposite direction.

4. Summary and Discussion

The results present a story which begins with a system that is bound almost exclusively by a common pnicogen bond to a π-donor. This complex obeys the standard rule wherein the bond is strengthened by enlargement of the pnicogen atom, making it more electropositive and polarizable. It is composed of electrostatic attraction as its prime ingredient, but also contains a fairly large amount of dispersion energy due to the proximity of the loose π-electron cloud of the donor.

As electron-withdrawing F and C≡N substituents replace the H atoms of ethylene, density is drawn away from the π-region, reversing its potential from negative to positive. This reversal causes a degree of repulsion with the σ-hole of the ZCl_3 molecule, cutting into the strength of the

pnicogen bond. But this bond weakening is compensated by a rise in the dispersive attraction, particularly for CN substituents where the dispersion energy is four to seven times larger than the electrostatic component. Another strengthening factor arises from noncovalent bonds between the two peripheral Cl atoms of ZCl_3 and the electronegative substituents on the ethylene, whether F or CN. These bonds are of comparable strength to the pnicogen bond for $C_2(CN)_4$ and their presence, including also a pair of bonds between Cl and the C=C midpoint of the alkene, helps to account for its very large interaction energies.

An NBO orbital picture of the interaction verifies the finding that the pnicogen bond weakens as the H atoms of ethylene are replaced by F or CN. This model attributes the secondary bonds to interactions between the peripheral Cl lone pairs and the C=C π^* antibonding orbital. The latter represent charge flow from ZCl_3 to alkene, opposite to the direction due to the pnicogen bond. As the pnicogen bond weakens in the alkene substituent order H > F > CN, the overall charge flow goes from alkene to ZCl_3 for ethylene, but is reversed for $C_2(CN)_4$.

In summary, there are two sorts of noncovalent bond present in these complexes between ZCl_3 and an alkene. In addition to a π-donor pnicogen bond, there are also bonds involving the lone pairs of the Cl atoms and the π^*(C=C) antibonding orbital. For unsubstituted ethylene, it is the former pnicogen bond that dominates the interaction. When the four H atoms of ethylene are replaced by C≡N, the latter lp-π bonds play the dominant role, supplemented by bonds between the Cl atoms and the substituents. To this, is added a large contribution from dispersion energy. The C_4F_4 alkene represents a middle ground, where both sorts of interactions make comparable contributions. The pnicogen bond is weaker than in C_2H_4, and the LP_{Cl}-π interactions are weaker than in $C_2(CN)_4$. As a result, the total interaction energy of C_4F_4 is smaller than in either of the other two cases.

It should be stressed that these results demonstrate that there is more to an intermolecular interaction than a simple consideration of MEPs. Such a view might explain the complexation results for C_2H_4, and how it varies with changing Z atom. But the diagrams in Fig 1 would lead one to suppose that the substituted alkenes ought to repel an incoming ZCl_3 molecule by simple Coulombic arguments. Indeed, the values of $V_{s,max}$ for $C_2(CN)_4$ and $SbCl_3$ are +0.064 and +0.032 au, respectively, quite large, translating to 40 and 20 kcal/mol. The ability of binding forces other than the pnicogen bond to pull these two subunits together against such a strong repulsion is certainly notable. So MEPs alone would not predict a stable complex, much less the

very strong forces that make the complexes involving $C_2(CN)_4$ even stronger than those including the unsubstituted ethylene.

Note also that this transition from one sort of primary interaction for C_2H_4, the pnicogen bond, to another dominated by lone pair-π attractions in $C_2(CN)_4$, comes with only minor changes in the overall molecular geometry of the complex. This similarity serves as a caution that one should be careful in taking the structure as the primary means of deciding which sort of noncovalent bond might be the dominant one.

The ability of the ZCl_3 molecules to bind to the C_2R_4 substituted alkenes, despite the Coulombic repulsion between areas of positive potential on the two subunits, does have some parallels in the literature. For example, pairs of benzene molecules can approach one another in a parallel, face-to-face fashion, although their quadrupole moments oppose such a geometry. The electrostatic repulsion is countered by a strong dispersion attraction between the two π-systems. However, the total interaction energy is less than 8 kJ/mol,[63-64] only a fraction of the 20-25 kJ/mol encountered here for the $C_2(CN)_4$ complexes with ZCl_3. Another example of a system overcoming electrostatic repulsion is the recently discussed set of "anti-electrostatic" H-bonds.[65-72] However, these interactions between ions of like charge are only metastable in the sense that they are less stable than the separated monomers.

Acknowledgment

This work was supported by the National Natural Science Foundation of China (21573188).

References

1. Batail, P.; Grandjean, D.; Dudragne, F.; Michaud, C. Etude Structurale De Fluoramines Aromatiques. II. Structure Cristalline Et Moléculaire Du (N,N-Difluoroamino) Trinitro-2,4,6 Benzène, $C_6H_2O_6N_4F_2$. *Acta Cryst.* **1975,** *B34*, 1367-1372.
2. Baker, W. A.; Williams, D. E. Antimony Trichloride 2:1 Complex with 1,3,5-Triacetylbenzene. *Acta Cryst.* **1978,** *B34*, 3739–3741.
3. Klinkhammer, K. W.; Pyykko, P. Ab Initio Interpretation of the Closed-Shell Intermolecular E···E Attraction in Dipnicogen $(H_2e\text{-}Eh_2)_2$ and $(He\text{-}Eh)_2$ Hydride Model Dimers. *Inorg. Chem.* **1995,** *34*, 4134-4138.
4. Carré, F.; Chuit, C.; Corriu, R. J. P.; Monforte, P.; Nayyar, N. K.; Reyé, C. Intramolecular Coordination at Phosphorus: Donor-Acceptor Interaction in Three- and Four-Coordinated Phosphorus Compounds. *J. Organomet. Chem.* **1995,** *499*, 147-154.
5. Avtomonov, E. V.; Megges, K.; Wocadlo, S.; Lorberth, J. Syntheses and Structures of Cyclopentadienyl Arsenic Compounds Part I: Pentamethylcylopentadienyl Arsenic Dihalides (Cp^*AsX_2,X=F, Cl, Br, I). *J. Organomet. Chem.* **1996,** *524*, 253-261.
6. Deiters, J. A.; Holmes, R. R. Ab Initio Treatment of a Phosphorus Coordinate, Trigonal Bipyramidal to Pentafluoride-Pyridine Reaction Square Pyramidal to Octahedral. *Phos. Sulf.*

Si, Rel. Elem. **1997,** *123*, 329-340.
7. Muller, G.; Brand, J.; Jetter, S. E. Donor-Acceptor Complexes between Organoamines and Phosphorus Tribromide. *Z. Naturforsch., B: Chem. Sci.* **2001,** *56*, 1163-1171.
8. Kilian, P.; Slawin, A. M. Z.; Woollins, J. D. Naphthalene-1,8-Diyl Bis(Halogenophosphanes): Novel Syntheses and Structures of Useful Synthetic Building Blocks. *Chem. Eur. J.* **2003,** *9*, 215-222.
9. Wang, W.; Zheng, W.; Pu, X.; Wong, N. ; Tian, A. An Ab Initio Study of P–H···P Interactions Using the Ph_3···Ph_3 Model Complex. *J. Mol. Struct. (Theochem)* **2003,** *625*, 25-30.
10. Szymczak, J. J.; Grabowski, S. J.; Roszak, S.; Leszczynski, J. H···Σ Interactions – an Ab Initio and `Atoms in Molecules' Study. *Chem. Phys. Lett.* **2004,** *393*, 81-86.
11. Bushuk, S. B.; Carré, F. H.; Guy, D. M. H.; Douglas, W. E.; Kalvinkovskya, Y. A.; Klapshina, L. G.; Rubinov, A. N.; Stupak, A. P.; Bushuk, B. A. Hypercoordinate Silicon and Phosphorus Acetylene Compounds: Crystal Structure Determinations and Fluorescence Spectroscopic Study. *Polyhedron* **2004,** *23*, 2615-2623.
12. Tschirschwitz, S.; Lonnecke, P.; Hey-Hawkins, E. Aminoalkylferrocenyldichlorophosphanes: Facile Synthesis of Versatile Chiral Starting Materials. *Dalton Trans.* **2007**, 1377-13782.
13. Vickaryous, W. J.; Healey, E. R.; Berryman, O. B.; Johnson, D. W. Synthesis and Characterization of Two Isomeric, Self-Assembled Arsenic− Thiolate Macrocycles. *Inorg. Chem.* **2005,** *44*, 9247-9252.
14. Cangelosi, V. M.; Zakharov, L. N.; Crossland, J. L.; Franklin, B. C.; Johnson, D. W. A Surprising “Folded-in” Conformation of a Self-Assembled Arsenic-Thiolate Macrocycle. *Cryst. Growth Des.* **2010,** *10*, 1471-1473.
15. Cangelosi, V. M.; Pitt, M. A.; Vickaryous, W. J.; Allen, C. A.; Zakharov, L. N.; Johnson, D. W. Design Considerations for the Group VI Elements: The Pnictogen···Π Interaction as a Complementary Component in Supramolecular Assembly Design. *Cryst. Growth Des.* **2010,** *10*, 3531-3536.
16. Solimannejad, M.; Gharabaghi, M.; Scheiner, S. SH···N and SH···P Blue-Shifting H-Bonds and N···P Interactions in Complexes Pairing HSN with Amines and Phosphines. *J. Chem. Phys.* **2011,** *134*, 024312.
17. Scheiner, S. A New Noncovalent Force: Comparison of P···N Interaction with Hydrogen and Halogen Bonds. *J. Chem. Phys.* **2011,** *134*, 094315.
18. Scheiner, S. Effects of Multiple Substitution Upon the P···N Noncovalent Interaction. *Chem. Phys.* **2011,** *387*, 79-84.
19. Li, Q.Z.; Li, R.; Liu, X.F.; Li, W.Z.; Cheng, J.B. Concerted Interaction between Pnicogen and Halogen Bonds in XCl···FH_2P···NH_3 (X=F, OH, CN, NC, and FCC). ChemPhysChem **2012**, *13*, 1205-1212.
20. Zahn, S.; Frank, R.; Hey-Hawkins, E.; Kirchner, B. Pnicogen Bonds: A New Molecular Linker? *Chem. Eur. J.* **2011,** *17*, 6034-6038.
21. Scheiner, S. Effects of Substituents Upon the P···N Noncovalent Interaction: The Limits of Its Strength. *J. Phys. Chem. A* **2011,** *115*, 11202-11209.
22. Sanchez-Sanz, G.; Trujillo, C.; Solimannejad, M.; Alkorta, I.; Elguero, J. Orthogonal Interactions between Nitryl Derivatives and Electron Donors: Pnictogen Bonds. *Phys. Chem. Chem. Phys.* **2013,** *15*, 14310-14318.
23. Alkorta, I.; Elguero, J.; Del Bene, J. E. Pnicogen Bonded Complexes of PO_2X (X = F, Cl) with Nitrogen Bases. *J. Phys. Chem. A* **2013,** *117*, 10497-10503.

24. Li, Q.Z.; Li, R.; Liu, X.F.; Li, W.Z.; Cheng, J.B. Pnicogen−Hydride Interaction between FH_2X (X = P and As) and HM (M = ZnH, BeH, MgH, Li, and Na). *J. Phys. Chem. A* **2012,** *116*, 2547-2553.
25. Alkorta, I.; Elguero, J.; Solimannejad, M. Single Electron Pnicogen Bonded Complexes. *J. Phys. Chem. A* **2014,** *118*, 947-953.
26. Zhuo, H.; Li, Q. Novel Pnicogen Bonding Interactions with Silylene as an Electron Donor: Covalency, Unusual Substituent Effects and New Mechanisms. *Phys. Chem. Chem. Phys.* **2015,** *17*, 9153-9160.
27. Ramanathan, N.; Sankaran, K.; Sundararajan, K. PCl_3-C_6H_6 Heterodimers: Evidence for P···π Phosphorus Bonding at Low Temperatures. *Phys. Chem. Chem. Phys.* **2016,** *18*, 19350-19358.
28. Bauza, A.; Quinonero, D.; Deya, P. M.; Frontera, A. Pnicogen-π Complexes: Theoretical Study and Biological Implications. *Phys. Chem. Chem. Phys.* **2012,** *14*, 14061-14066.
29. Scheiner, S.; Adhikari, U. Abilities of Different Electron Donors (D) to Engage in a P...D Noncovalent Interaction. *J. Phys. Chem. A* **2011,** *115*, 11101-11110.
30. An, X. ; Li, R.; Li, Q. ; Liu, X. ; Li, W.; Cheng, J. Substitution, Cooperative, and Solvent Effects on π Pnicogen Bonds in the FH_2P and FH_2As Complexes. *J. Mol. Model.* **2012,** *18*, 4325-4332.
31. Egli, M.; Sarkhel, S. J. Lone Pair−π Aromatic Interactions: To Stabilize or Not to Stabilize. *Acc. Chem. Res.* **2007,** *40*, 197-205.
32. Estarellas, C.; Frontera, A.; Quinonero, D.; Deya, P. M. Anion-π Interactions in Flavoproteins. *Chem. Asian J.* **2011,** *6*, 2316-2318.
33. Lucas, X.; Bauza, A.; Frontera, A.; Quinonero, D. A Thorough Anion-π Interaction Study in Biomolecules: On the Importance of Cooperativity Effects. *Chem. Sci.* **2016,** *7*, 1038-1050.
34. Mooibroek, T. J.; Gamez, P.; Reedijk, J. Lone Pair–π Interactions: A New Supramolecular Bond? *CrystEngComm* **2008,** *10*, 1501-1515.
35. Singh, S. K.; Das, A. The N → π* Interaction: A Rapidly Emerging Non-Covalent Interaction. *Phys. Chem. Chem. Phys.* **2015,** *17*, 9596-9612.
36. Wilson, K. A.; Kellie, J. L.; Wetmore, S. D. DNA-Protein π-Interactions in Nature: Abundance, Structure, Composition and Strength of Contacts between Aromatic Amino Acids and DNA Nucleobases or Deoxyribose Sugar. *Nucleic Acids Res.* **2014,** *42*, 6726-6741.
37. Estarellas, C.; Frontera, A.; Quinonero, D.; Deya, P. M. Relevant Anion-π Interactions in Biological Systems: The Case of Urate Oxidase. *Angew. Chem. Int. Ed.* **2011,** *50*, 415-418.
38. Bartlett, G. J.; Choudhary, A.; Raines, R. T.; Woolfson, D. N. N→π* Interactions in Proteins. *Nat. Chem. Biol.* **2010,** *6*, 615-620.
39. Stollar, E. J.; Gelpi, J. L.; Velankar, S.; Golovin, A.; Orozco, M.; Luisi, B. F. Unconventional Interactions between Water and Heterocyclic Nitrogens in Protein Structures. *Proteins* **2004,** *57*, 1-8.
40. Bauza, A.; Quinonero, D.; Deya, P. M.; Frontera, A. Long-Range Effects in Anion-π Interactions: Their Crucial Role in the Inhibition Mechanism of Mycobacterium Tuberculosis Malate Synthase. *Chem. Eur. J.* **2014,** *20*, 6985-6990.
41. Egli, M.; Gessner., R. V. Stereoelectronic Effects of Deoxyribose O4'on DNA Conformation. *Pro. Natl. Acad. Sci.* **1995,** *92*, 180-184.
42. Kozelka, J. Lone Pair-π Interactions in Biological Systems: Occurrence, Function, and Physical Origin. *Euro. Biophys. J.* **2017,** *46*, 729-737.

43. Berger, G.; Soubhye, J.; van der Lee, A.; Vande Velde, C.; Wintjens, R.; Dubois, P.; Clément, S.; Meyer, F. Interplay between Halogen Bonding and Lone Pair-π Interactions: A Computational and Crystal Packing Study. *ChemPlusChem* **2014,** *79*, 552-558.
44. Korenaga, T.; Shoji, T.; Onoue, K.; Sakai, T. Demonstration of the Existence of Intermolecular Lone Pair···π Interaction between Alcoholic Oxygen and the C_6F_5 Group in Organic Solvent. *Chem. Commun.* **2009**, *31*, 4678-4680.
45. Geboes, Y.; De Proft, F.; Herrebout, W. A. Lone Pair···π Interactions Involving an Aromatic π-System: Complexes of Hexafluorobenzene with Dimethyl Ether and Trimethylamine. *Chem. Phys. Lett.* **2016,** *647*, 26-30.
46. Geboes, Y.; De Proft, F.; Herrebout, W. A. Expanding Lone Pair...π Interactions to Nonaromatic Systems and Nitrogen Bases: Complexes of C_2F_3X (X = F, Cl, Br, I) and Tma-d_9. *J. Phys. Chem. A* **2015,** *119*, 5597-5606.
47. Bauzá, A.; Frontera, A. Competition between Lone Pair-π, Halogen-π and Triel Bonding Interactions Involving BX_3 (X=F, Cl, Br and I) Compounds: An Ab Initio Study. *Theor. Chem. Acc.* **2017,** *136*, 37.
48. Wang, L.; Zhou, H.; Yang, T.; Ke, H.; Tu, Y. ; Yao, H.; Jiang, W. Bis-Naphthalene Cleft with Aggregation-Induced Emission Properties through Lone-Pair···π Interactions. *Chem. Eur. J.* **2018,** *24*, 16757-16761.
49. Ran, J.; Hobza, P. On the Nature of Bonding in Lone Pair···π-Electron Complexes: CCSD(T)/Complete Basis Set Limit Calculations. *J. Chem. Theory Comput.* **2009,** *5*, 1180-1185.
50. Reyes, A.; Fomina, L.; Rumsh, L.; Fomine, S. Are Water-Aromatic Complexes Always Stabilized Due to π-H Interactions? LMP2 Study. *Int. J. Quantum Chem.* **2005,** *104*, 335-341.
51. Feller, D. The Role of Databases in Support of Computational Chemistry Calculations. *J. Comput. Chem.* **1996,** *17*, 1571-1586.
52. Boys, S. F.; Bernardi, F. D. The Calculation of Small Molecular Interactions by the Differences of Separate Total Energies. Some Procedures with Reduced Errors. *Mol. Phys.* **1970,** *19*, 553-566.
53. Frisch, M. J.; Trucks, G. W.; Schlegel, H. B.; Scuseria, G. E.; Robb, M. A.; Cheeseman, J. R.; Scalmani, G.; Barone, V.; Mennucci, B.; Petersson, G. A.; et al. Gaussian 09, Revision B.01; Gaussian Inc.: Wallingford, CT, 2009.
54. Bulat, F. A.; Toro-Labbé, A.; Brinck, T.; Murray, J. S.; Politzer, P. Quantitative Analysis of Molecular Surfaces: Areas, Volumes, Electrostatic Potentials and Average Local Ionization Energies. *J. Mol. Model.* **2010,** *16*, 1679-1691.
55. Bader, R. Aim2000 Program, V. 2.0. *McMaster University, Hamilton, Canada* **2000**.
56. Reed, A. E.; Curtiss, L. A.; Weinhold, F. Intermolecular Interactions from a Natural Bond Orbital, Donor-Acceptor Viewpoint. *Chem. Rev.* **1988,** *88*, 899-926.
57. Lu, T.; Chen, F. Multiwfn: A Multifunctional Wavefunction Analyzer. *J. Comput. Chem.* **2012,** *33*, 580-592.
58. Humphrey, W.; Dalke, A.; Schulten, K. Vmd: Visual Molecular Dynamics. *J. Mol. Graph.* **1996,** *14*, 33-38.
59. Su, P.; Li, H. Energy Decomposition Analysis of Covalent Bonds and Intermolecular Interactions. *J. Chem. Phys.* **2009,** *131*, 014102.
60. Schmidt, M. W.; Baldridge, K. K.; Boatz, J. A.; Elbert, S. T.; Gordon, M. S.; Jensen, J. H.; Koseki, S.; Matsunaga, N.; Nguyen, K. A.; Su, S. General Atomic and Molecular Electronic

Structure System. *J. Comput. Chem.* **1993,** *14*, 1347-1363.
61. Johnson, E. R.; Keinan, S.; Mori-Sanchez, P.; Contreras-García, J.; Cohen, A. J.; Yang, W. Revealing Noncovalent Interactions. *J. Am. Chem. Soc.* **2010,** *132*, 6498-6506.
62. Contreras-García, J.; Johnson, E. R.; Keinan, S.; Chaudret, R.; Piquemal, J.-P.; Beratan, D. N.; Yang, W. Nciplot: A Program for Plotting Noncovalent Interaction Regions. *J. Chem. Theory Comput.* **2011,** *7*, 625-632.
63. Lee, E. C.; Kim, D.; Jurečka, P.; Tarakeshwar, P.; Hobza, P.; Kim, K. S. Understanding of Assembly Phenomena by Aromatic−Aromatic Interactions: Benzene Dimer and the Substituted Systems. *J. Phys. Chem. A* **2007,** *111*, 3446-3457.
64. Bettinger, H. F.; Kar, T.; Sánchez-García, E. Borazine and Benzene Homo- and Heterodimers. *J. Phys. Chem. A* **2009,** *113*, 3353-3359.
65. Iribarren, Í.; Montero-Campillo, M. M.; Alkorta, I.; Elguero, J.; Quiñonero, D. Cations Brought Together by Hydrogen Bonds: The Protonated Pyridine–Boronic Acid Dimer Explained. *Phys. Chem. Chem. Phys.* **2019,** *21*, 5796-5802.
66. Barbas, R.; Prohens, R.; Bauzá, A.; Franconetti, A.; Frontera, A. H-Bonded Anion–Anion Complexes in Fentanyl Citrate Polymorphs and Solvates. *Chem. Commun.* **2019,** *55*, 115-118.
67. Wang, C.; Fu, Y.; Zhang, L.; Danovich, D.; Shaik, S.; Mo, Y. Hydrogen- and Halogen-Bonds between Ions of Like Charges: Are They Anti-Electrostatic in Nature? *J. Comput. Chem.* **2018,** *39*, 481-487.
68. Chalanchi, S. M.; Alkorta, I.; Elguero, J.; Quiñonero, D. Hydrogen Bond Versus Halogen Bond in Cation–Cation Complexes: Effect of the Solvent. *ChemPhysChem* **2017,** *18*, 3462-3468.
69. Quinonero, D.; Alkorta, I.; Elguero, J. Cation-Cation and Anion-Anion Complexes Stabilized by Halogen Bonds. *Phys. Chem. Chem. Phys.* **2016,** *18*, 27939-27950.
70. Alkorta, I.; Mata, I.; Molins, E.; Espinosa, E. Charged Versus Neutral Hydrogen-Bonded Complexes: Is There a Difference in the Nature of the Hydrogen Bonds? *Chem. Eur. J.* **2016,** *22*, 9226-9234.
71. Weinhold, F.; Klein, R. A. Anti-Electrostatic Hydrogen Bonds. *Angew. Chem. Int. Ed.* **2014,** *53*, 11214-11217.
72. Mata, I.; Molins, E.; Alkorta, I.; Espinosa, E. The Paradox of Hydrogen-Bonded Anion–Anion Aggregates in Oxoanions: A Fundamental Electrostatic Problem Explained in Terms of Electrophilic···Nucleophilic Interactions. *J. Phys. Chem. A* **2014,** *119*, 183-194.

Table 1. Interaction energy (E^{int}, kJ/mol), distances (R, Å)[a] and angles (degs) in $C_2R_4\cdots ZCl_3$

	E^{int}	R_1	R_2	R_3	R_2-R_3	α	β
$C_2H_4\cdots PCl_3$	-12.28	3.341	3.477	3.209	0.268	84.0	165.7
$C_2H_4\cdots AsCl_3$	-15.53	3.249	3.407	3.145	0.262	82.3	166.9
$C_2H_4\cdots SbCl_3$	-19.67	3.225	3.372	3.122	0.250	82.6	170.2
$C_2F_4\cdots PCl_3$	-10.61	3.201	3.373	3.372	0.001	93.4	167.1
$C_2F_4\cdots AsCl_3$	-9.89	3.210	3.335	3.385	0.050	92.4	170.4
$C_2F_4\cdots SbCl_3$	-9.10	3.294	3.312	3.392	0.080	91.7	176.2
$C_2(CN)_4\cdots PCl_3$	-24.68	3.230	3.394	3.396	0.002	97.5	172.6
$C_2(CN)_4\cdots AsCl_3$	-22.81	3.353	3.360	3.371	0.011	99.2	176.3
$C_2(CN)_4\cdots SbCl_3$	-21.87	3.491	3.353	3.355	0.002	100.7	167.2

[a]R_1 is the distance between C_1 and Z, while R_2 and R_3 are respectively the distances from C_2 to Cl_2 and Cl_3.

Table 2. Electrostatic (E^{ele}), exchange (E^{ex}), repulsion (E^{rep}), polarization (E^{pol}), and dispersion (E^{disp}) energy components in $C_2R_4\cdots ZCl_3$, all in kJ/mol

	$E^{ele,a}$	E^{ex}	E^{rep}	E^{pol}	E^{disp}
$C_2H_4\cdots PCl_3$	-22.91(43%)	-58.98	99.44	-7.36(14%)	-22.95(43%)
$C_2H_4\cdots AsCl_3$	-35.36(47%)	-81.34	140.74	-12.92(17%)	-26.92(36%)
$C_2H_4\cdots SbCl_3$	-48.24(48%)	-107.68	188.39	-23.03(23%)	-29.18(29%)
$C_2F_4\cdots PCl_3$	-11.87(26%)	-46.19	80.21	-5.68(13%)	-27.55(61%)
$C_2F_4\cdots AsCl_3$	-10.99(23%)	-48.95	85.86	-7.15(15%)	-28.97(62%)
$C_2F_4\cdots SbCl_3$	-10.49(20%)	-55.55	97.90	-10.16(20%)	-30.89(60%)
$C_2(CN)_4\cdots PCl_3$	-13.33(17%)	-76.03	131.08	-12.46(16%)	-54.67(67%)
$C_2(CN)_4\cdots AsCl_3$	-9.78(13%)	-76.54	131.63	-12.21(16%)	-56.43(71%)
$C_2(CN)_4\cdots SbCl_3$	-7.98(10%)	-80.55	138.36	-13.67(17%)	-58.23(73%)

[a]values in parentheses are the percentage of E^{ele}, E^{pol} and E^{disp} to the sum of these three terms.

Table 3. Electron density (ρ), Laplacian ($\nabla^2\rho$), and energy density (H) at the intermolecular BCP, all in au.

	ρ	$\nabla^2\rho$	H
$C_2H_4\cdots PCl_3$	0.0095	0.0246	0.0009
$C_2H_4\cdots AsCl_3$	0.0124	0.0284	0.0006
$C_2H_4\cdots SbCl_3$	0.0151	0.0295	0.0001
$C_2F_4\cdots PCl_3$	0.0107	0.0287	0.0006
$C_2F_4\cdots AsCl_3$	0.0114	0.0285	0.0005
$C_2F_4\cdots SbCl_3$	0.0118	0.0263	0.0003
$C_2(CN)_4\cdots PCl_3$	0.0098	0.0290	0.0009
$C_2(CN)_4\cdots AsCl_3$	0.0077	0.0240	0.0009
$C_2(CN)_4\cdots SbCl_3$	0.0068	0.0209	0.0009

Table 4. Electron density (ρ), Laplacian ($\nabla^2\rho$), and energy density (H) at the intermolecular BCP of secondary interactions, all in au.

	$Cl_2\cdots R^a$			$Cl_3\cdots R$		
	ρ	$\nabla^2\rho$	H	ρ	$\nabla^2\rho$	H
$C_2F_4\cdots PCl_3$	0.0048	0.0209	0.0011	0.0048	0.0211	0.0011
$C_2F_4\cdots AsCl_3$	0.0046	0.0198	0.0010	0.0053	0.0233	0.0012
$C_2F_4\cdots SbCl_3$	0.0046	0.0194	0.0010	0.0056	0.0241	0.0012
$C_2(CN)_4\cdots PCl_3$	0.0063	0.0236	0.0013	0.0064	0.0237	0.0013
$C_2(CN)_4\cdots AsCl_3$	0.0066	0.0246	0.0013	0.0067	0.0251	0.0013
$C_2(CN)_4\cdots SbCl_3$	0.0066	0.0246	0.0013	0.0068	0.0252	0.0013
	$Cl_2\cdots C_1\text{-}C_2{}^b$			$Cl_3\cdots C_1\text{-}C_2$		
$C_2(CN)_4\cdots AsCl_3$	0.0063	0.0223	0.0013	0.0065	0.0226	0.0013
$C_2(CN)_4\cdots SbCl_3$	0.0061	0.0211	0.0012	0.0064	0.0218	0.0012

[a]R=F atom for C_2F_4 and C atom of CN for $C_2(CN)_4$
[b]approximate midpoint of C_1-C_2 bond

Table 5. Charge transfer (CT, e) and second-order perturbation energies[a] (E, kJ/mol) in $C_2R_4\cdots ZCl_3$.

	CT	E_1	E_2	E_3	E_4	E_5
$C_2H_4\cdots PCl_3$	-0.0035	13.04	---	0.29	1.76	4.35
$C_2H_4\cdots AsCl_3$	-0.0121	23.62	0.38	0.67	2.01	5.52
$C_2H_4\cdots SbCl_3$	-0.0241	34.44	2.51	3.30	3.01	6.77
$C_2F_4\cdots PCl_3$	-0.0099	10.37	0.29	0.29	2.42	0.38
$C_2F_4\cdots AsCl_3$	-0.0132	14.00	0.42	0.29	2.42	0.92
$C_2F_4\cdots SbCl_3$	-0.0172	16.72	1.46	1.05	2.42	1.17
$C_2(CN)_4\cdots PCl_3$	0.0218	3.30	0.25	0.25	3.85	0.21
$C_2(CN)_4\cdots AsCl_3$	0.0188	1.96	0.25	0.25	2.09	0.00
$C_2(CN)_4\cdots SbCl_3$	0.0189	1.00	0.42	0.38	1.46	0.00

[a]E_1, E_2, E_3, E_4, and E_5 correspond to the orbital interactions of $\pi_{C=C}\rightarrow\sigma^*_{Z\text{-}Cl1}$, $\pi_{C=C}\rightarrow\sigma^*_{Z\text{-}Cl2}$, $\pi_{C=C}\rightarrow\sigma^*_{Z\text{-}Cl3}$, $Lp_Z\rightarrow\pi^*_{C=C}$, $Lp_{Cl3}\rightarrow\pi^*_{C=C}$, respectively.

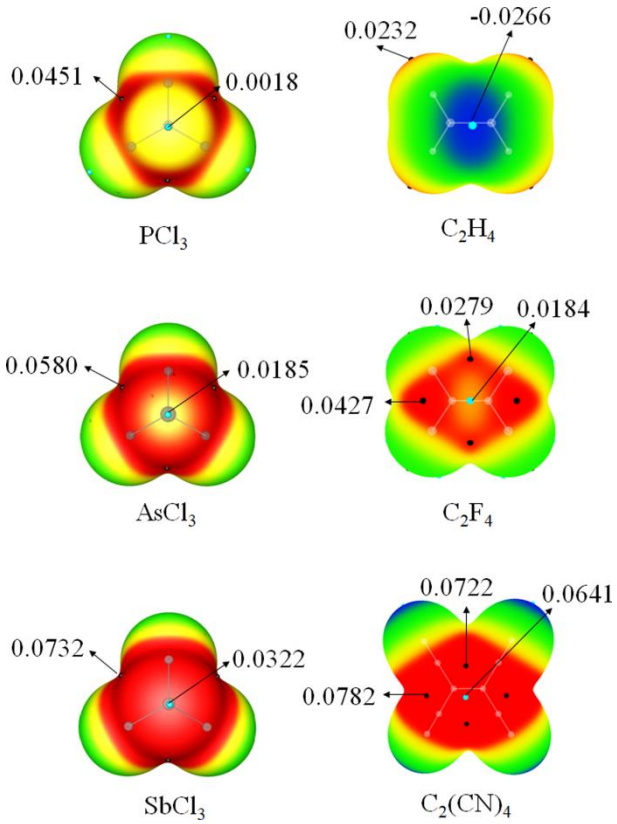

Figure 1 MEP maps of ZCl_3 (Z=P, As, Sb) and C_2X_4 (X= H, F and CN). Color ranges, in au are: red, greater than 0.02; yellow, between 0.02 and 0; green, between 0 and -0.02; blue, smaller than -0.02.

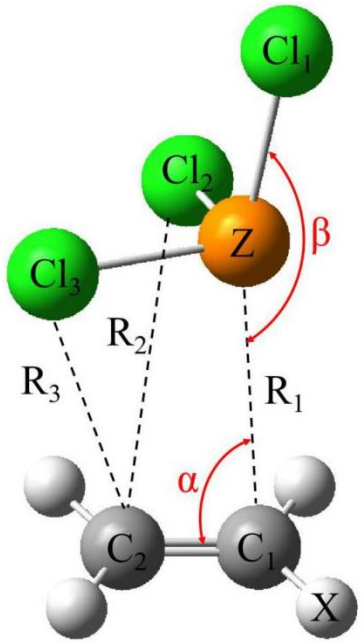

Figure 2 Schematic diagram of molecular structure of complex